Inorg. Chem. **2006**, *45*, 8062–8069

Organic–Inorganic Hybrid Compounds of Li with Bisimidazole Derivatives: Li Ion Binding Study and Topochemical Properties

In-Chul Hwang,* R. Prakash Chandran, N. Jiten Singh, Manish Khandelwal, T. Daniel Thangadurai, Jung-Woo Lee, Jeong Ah Chang, and Kwang S. Kim*

Center for Superfunctional Materials, Department of Chemistry, Pohang University of Science and Technology, Pohang 790-784, Korea

Received February 24, 2006

The imidazole-based ligands, bis(imidazol-1-yl)methane (Bizm, **1a**) and (pyrenyl)bis(imidazol-1-yl) methane (Pbizm, **2a**) were prepared. With $LiClO_4$, these two compounds formed two novel organic–inorganic hybrid materials: a 3D network polymer $Li(Bizm)\cdot ClO_4$ (**1b**) and a 1D chain polymer $Li(Pbizm)_2\cdot ClO_4$ (**2b**). The intriguing topological and physiochemical characteristics of **1b** and **2b** are reported on the basis of the X-ray single-crystal structure analysis and Li ion binding studies.

I. Introduction

The design and synthesis of molecular inorganic−organic hybrid materials is an area of hot pursuit because of their distinctive topology and functional architectural frameworks and potential applications in energy storage devices, catalysis, etc.[1−3] There is a wealth of information available on coordination polymers with metal ion connectors and organic linkers incorporated into their frameworks, which may be attributed to their distinctive topology, as well as to their utility.[4−8] Although the neutral ditopic nitrogen-containing ligands, such as pyrazine, 4,4′-bipyridine, and 1,10-phenanthroline, have been extensively employed,[6,9−16] the scope of preparing coordination polymers from the ditopic bisimidazoles remains largely unexplored. Recently, efforts have been made to incorporate bisimidazolium into naphthalene and pyridine macrocyclic calix structures, which function as anion receptors.[17−19] Imidazole−lithium complexes are also of importance because they have applications in electrical devices, olefin polymerizations, etc.[20−22] Room-temperature ionic liquids derived from imidazole, being nonflammable and nonvolatile, are widely employed as conductive nonaqueous electrolytes in high-power-density lithium batteries.[23] Recently, lithium salts of imidazole with weakly coordinating anions have been reported as organic electrolytes.[22]

* To whom correspondence should be addressed. E-mail: spfe@postech.ac.kr (I.-C.H.); kim@postech.ac.kr (K.S.K.).

(1) Hagrman, P. J.; Hagrman, D.; Zubieta, J. *Angew. Chem., Int. Ed. Engl.* **1999**, *38*, 2638−2684.
(2) Kitagawa, S.; Kitaura, R.; Noro, S. *Angew. Chem., Int. Ed.* **2004**, *43*, 2334−2375.
(3) Herrmann, W. A.; Goossen, L. J.; Spiegler, M. *Organometallics* **1998**, *17* (11), 2162−2168.
(4) Ramprasad, D.; Pez, G. P.; Toby, B. H.; Markley, T. J.; Pearlstein, R. M. *J. Am. Chem. Soc.* **1995**, *117*, 10694−10701.
(5) Munakata, M.; Wu, L. P.; Kuroda-Sowa, T. T.; Suenaga, Y.; Sugimoto, K. *Inorg. Chem.* **1997**, *36*, 4903−4905.
(6) Oh, M. H.; Carpenter, G. B.; Sweigart, D. A. *Angew. Chem., Int. Ed.* **2002**, *41*, 3650−3653.
(7) Liu, X.; Guo, G.; Liu, B.; Chen, W.; Huang, J. *Cryst. Growth Des.* **2005**, *5*, 841−843.
(8) Ghassemzadeh, M.; Heravi, M.; Hekmat-Shoar, R.; Neumueller, B. *Z. Anorg. Allg. Chem.* **2003**, *629*, 2438−2439.
(9) Hoskins, B. F.; Robson, R.; Slizys, D. A. *J. Am. Chem. Soc.* **1997**, *119*, 2952−2953.
(10) Ma, J.; Yang, J.; Zheng, G.; Li, L.; Zhang, Y.; Li, F.; Liu, J. *Polyhedron* **2004**, *23*, 553−559.
(11) Fan, J.; Sun, W.; Okamura, T.; Zheng, Y.; Sui, B.; Tang, W.; Ueyama, N. *Cryst. Growth Des.* **2004**, *4*, 579−584.
(12) Ma, J.; Yang, J.; Zheng, G.; Li, L.; Liu, J. *Inorg. Chem.* **2003**, *42*, 7531−7534.
(13) Ma, J.; Liu, J.; Xing, Y.; Jia, H.; Lin, Y. *Dalton* **2000**, 2403−2407.
(14) Baylies, C. J.; Riis-Johannessen, T.; Harding, L. P.; Jeffery, J. C.; Moon, R.; Rice, C. R.; Whitehead, M. *Angew. Chem., Int. Ed.* **2005**, *44*, 6909−6912.
(15) Duncan, P. C. M.; Goodgame, D. M. L.; Menzer, S.; Williams, D. J. *Chem. Commun.* **1996**, 2127.
(16) Liu, X.; Guo, G.-C.; Wu, A.; Huang, J. *Inorg. Chem. Commun.* **2004**, *7*, 1261−1263.
(17) Chellappan, K.; Singh, N. J.; Hwang, I. C.; Lee, J. W.; Kim, K. S. *Angew. Chem., Int. Ed.* **2005**, *44*, 2899−2903.
(18) Ihm, H.; Yun, S.; Kim, H. G.; Kim, J. K.; Kim, K. S. *Org. Lett.* **2002**, *4*, 2897−2900.
(19) Yoon, J.; Kim, S. K.; Singh, N. J.; Kim K. S. *Chem. Soc. Rev.* **2006**, 355−360.
(20) LaPointe, R. E.; Roof, G. R.; Abboud, K. A.; Klosin, J. *J. Am. Chem. Soc.* **2000**, *122*, 9560−9561.
(21) Christie, M.; Lilley, S. J.; Staunton, E.; Andreev, Y. G. *Nature* **2005**, *433*, 50−53.
(22) Barbarich, T. J.; Driscoll, P. F.; Izquierdo, S.; Zakharov, L. N.; Incarvito, C. D.; Rheingold, A. L. *Inorg. Chem.* **2004**, *43*, 7764−7773.
(23) Fuller, J.; Carlin, R. T.; De Long, H. C.; Haworth, D. *Chem. Commun.* **1994**, 299−300.

10.1021/ic060323h CCC: $33.50
Published on Web 08/26/2006

Scheme 1

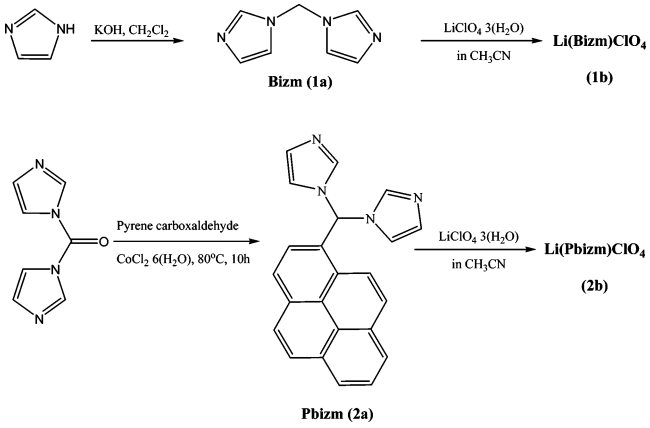

In this article, we discuss the synthesis, as well as the intriguing topology, of two coordination polymers derived from bisimidazole by complexation with $LiClO_4$ (see Scheme 1). We contemplate the utility of these versatile ligands in the fabrication of functional organic−inorganic hybrid materials. The initial investigations of their frameworks and thermal and electrochemical properties strongly indicate that these compounds are promising candidates for applications in electronic devices, organometallic framework design, and catalysis in the area of lithium chemistry.

II. Experimental Section

Apparatus and General Procedures. All reagents and solvents were available commercially. ^{1}H NMR and ^{13}C NMR spectra were performed on a Bruker ADVANCE-DPX500 (500 MHz) spectrometer at 298 K. The ^{7}Li NMR spectra was recorded on a Bruker AVANCE-DRX500 spectrometer with a standard Bruker double-tuned 4 mm probe: ^{7}Li 194.369 MHz. Chemical shifts of ^{7}Li NMR was externally referenced to 1 M $LiClO_4 \cdot 3(H_2O)$(in CH_3CN). TGA measurements were recorded on a TA Instruments TA 50 as a 5% weight loss temperature at a scan rate of 10 °C/min.

Electrochemical experiments for a conductivity measurement and cyclovoltammetry analysis were carried out using an EG & G PAR model 273A potentiostat/galvanostat interfaced with a computer. The ionic conductivity was measured in a typical conductivity cell with two platinum pellets as an electrode. Cyclic voltammograms were measured in a three-electrode cell using a 1.0 mm diameter glassy-carbon disk working electrode, a silver-wire reference electrode, and a platinum-gauze counter electrode. The potential was measured by cyclic voltammetry (CV) at room temperature in 0.4 M $[^nBu_4N][PF_6]/CH_3CN$.

High-resolution mass spectra were obtained on a Micromass Platform II mass spectrometer. Imidazole and pyrene carboxaldehyde were purchased from Aldrich.

Synthesis and Characterization of 1a and 2a. 1a was prepared according to the literature method[24,25] and sublimated for purification at 180 °C under high vacuum. The pyrenyl derivative **2a** was prepared by the reaction between pyrene carboxaldehyde (500 mg, 2 mmol), bis(imidazolyl)ketone (400 mg, 2 mmol), and $CoCl_2 \cdot 6(H_2O)$ (4 mg, 0.02 mmol) at 80 °C for 2 h. Subsequent column chromatography over silica gel using $CHCl_3$/MeOH (99:1 vol %) gave the compound as a fine white powder in a 60% yield (mp = 123 °C). ^{1}H NMR (500 MHz, $CDCl_3$): δ 8.45 (s, 1H), 8.31 (d, J = 7.4 Hz, 1H), 8.27 (d, J = 7.4 Hz, 1H), 8.20−8.16 (m, 3H), 8.11 (d, J = 7.8 Hz, 2H), 7.91 (d, J = 9.2 Hz, 1H), 7.60 (s, 2H), 7.34 (d, J = 8 Hz, 1H), 7.22 (s, 2H), 6.97 (s, 2H). ^{13}C NMR (125 MHz, $CDCl_3$): δ 137.3, 133.1, 130.8, 129.7, 129.5, 129.3, 128.9, 128.5, 127.7, 127.2, 126.8, 126.5, 126.3, 125.1,125.0, 124.4, 123.6, 121.1, 119.2, 68.5. ESI-MS: m/z 349.23 [M + H$^+$].

Crystallization of 1b and 2b. Colorless cubic crystals of **1b** and colorless needle crystals of **2b** were obtained by slow evaporation of a CH_3CN solution at room temperature. Also, identical crystals of **1b** and **2b** were obtained at various molar ratios ($LiClO_4$/**1a** and $LiClO_4$/**2a** = 4:1, 2:1, 1:1, 1:2, and 1:4) under the same conditions. After isolation of **1b** and **2b**, the excess of $LiClO_4 \cdot 3(H_2O)$ and **1a** or **2a** were characterized individually with X-ray single-crystal analysis and ^{1}H NMR spectroscopy.

Crystals of compound **1b** and **2b** were removed from the flask and covered with a layer of hydrocarbon oil. A suitable crystal was selected, attached to a glass fiber, and placed in the apparatus at the room temperature. Data for **1b** and **2b** were collected at 298-(2) K using a Bruker/Siemens SMART APEX instrument (Mo Kα radiation, λ = 0.71073 Å) equipped with a Cryocool NeverIce low-temperature device. Data were measured using ω and 2θ scans of 0.3° per frame for 10s, and a full sphere of data was collected. A total of 1380 frames were collected with a final resolution of 0.75 Å. The first 48 frames were recollected at the end of data collection to monitor for decay. Cell parameters were retrieved using SMART[26] software and refined using SAINT Plus[27] on all observed reflections. Data reduction and correction for Lp and decay were performed using the SAINT Plus software. Absorption corrections were applied using SADABS.[28] The structure was solved by direct methods and refined by full-matrix least-squares method on F^2 using the SHELXTL program package. All atoms were refined anisotropically, and hydrogen atoms were placed in calculated positions. No decomposition was observed during data collection. CIF files of the data collection and refinement are provided in the Supporting Information. Crystallographic data for the structures reported in this paper have been deposited with the Cambridge Crystallographic Data Centre. Detailed data collection and refinement of the two complexes are summarized in Table 1. Selected bond distances and angles are summarized in Table 2.

III. Results and Discussion

The coordination polymer $[Li(Bizm)]^+ \cdot [ClO_4]^-$ (**1b**) was prepared by a one-step reaction of $LiClO_4 \cdot 3(H_2O)$ and bis-(imidazol-1-yl)methane (Bizm, **1a**) in acetonitrile. The resulting solution afforded colorless cubic single crystals in excellent yield via crystallization. The crystals of **1b**, which were insoluble in acetonitrile, were dissolved easily in an acetonitrile/water (9:1) mixture. The addition of excess amounts of Bizm in acetonitrile also afforded $[Li(Bizm)]^+ \cdot [ClO_4]^-$ (**1b**) as the sole product.

The next attempt is to synthesize novel (pyrenyl)bis-(imidazole)methane (Pbizm, **2a**) introducing the delocalized π-electron system with $\pi-\pi$-facial topology[29] between attached imidazole- and pyrene-moieties, which would have

(24) Diez-Barra, E.; de la Hoz, A.; Sanchez-Migallon, A.; Tejeda, J. *Heterocycles* **1992**, *34* (7), 1365−1372.
(25) Viciano, M.; Mas-Marza, E.; Poyatos, M.; Sanau, M.; Crabtree, R. H.; Peris, E. *Angew. Chem., Int. Ed.* **2005**, *44*, 444−447.
(26) *SMART*, version 5.625; Bruker AXS: Madison, WI, 2001.
(27) *SAINTPlus*, version 6.22; Bruker AXS: Madison, WI, 2001.
(28) Sheldrick, G. M. *SADABS*, version 2.01; Bruker AXS: Madison, WI, 2001. (b) *SHELXTL*, version 6.10; Bruker AXS: Madison, WI, 2001.
(29) Kim, K. S.; Tarakeshwar, P.; Lee, J. Y. *Chem. Rev.* **2000**, *100*, 4145−4186.

Table 1. Crystallographic Data and Refinement Parameters for Li(Bimz)·ClO_4 (**1b**) and Li(Pbizm)·ClO_4 (**2b**)

	Li(Bimz)·ClO_4 (**1b**)	$Li(Pbizm)_2ClO_4$ (**2b**)
mol formula	$C_7H_8ClLiN_4O_4$	$C_{48}H_{35}ClLiN_9O_4$
fw	254.56	844.24
T (K)	293(2) K	293(2)
λ (Å)	0.71073	0.71073
cryst syst	tetragonal	orthorhombic
space group	$P4(1)$	$Abm2$
cryst size (mm^3)	0.1 × 0.1 × 0.1	0.30 × 0.10 × 0.10
a (Å)	9.151(2)	12.318(7)
b (Å)	9.151(2)	22.840(13)
c (Å)	13.023(5)	14.759(8)
V ($Å^3$)	1090.7(6)	4152(4)
Z	4	4
D_c (Mg/m^3)	1.550	1.350
μ (mm^{-1})	0.357	0.150
$F(000)$	520	1752
index ranges	$-9 \le h \le 11$	$-16 \le h \le 16$
	$-11 \le k \le 11$	$-29 \le k \le 26$
	$-16 \le l \le 15$	$-195 \le l \le 15$
reflns collected	6431	12 846
reflns independent	2181	4617
	$R(\text{int}) = 0.0293$	$R(\text{int}) = 0.0505$
data/restraints/params	2181/1/154	4617/1/294
GOF on F^2	0.967	0.911
absolute structure params	−0.02(8)	−0.19(13)
R1, wR2, $[I > 2\sigma(I)]^a$	0.0399, 0.0815	0.0600, 0.1619
R1, wR2, (all data)^a	0.0562, 0.0867	0.0996, 0.1765
$\Delta\rho_{min}$ and $\Delta\rho_{max}$ (e $Å^{-3}$)	0.242 and −0.148	0.613 and −0.402

^{a} $R1 = [\sum||F_o| - |F_c||/\sum|F_o|$; $wR2 = \{\sum[w(F_o^2 - F_c^2)^2]/\sum[w(F_o^2)^2]\}^{1/2}$; $w = 1/[\sigma^2(F_o^2) + (aP)^2 + bP]$, where $P = [2F_c^2 + \max(F_o^2,0)]/3$.

Table 2. Selected Bond Lengths (Å) and Angles (deg) for **1b** and **2b**^{a}

1b

Li−O(1)	2.003(8)	Li−N(1)	2.008(8)
Li−O(4′)#1	1.957(9)	Li−N(4′)#2	1.997(8)
Cl(1)−O(1)	1.433(4)	Cl(1)−O(3)	1.333(5)
Cl(1)−O(2)	1.355(6)	Cl(1)−O(4)	1.316(6)

O(4′)#1−Li−O(1)	95.8(5)	N(4′)#2−Li−N(1)	108.1(4)
O(4′)#1−Li−N(4′)#2	107.9(4)	O(4′)#1−Li−N(1)	105.4(5)
N(4′)#2−Li−O(1)	115.6(4)	O(1)−Li−N(1)	121.9(4)
Cl(1)−O(1)−Li	126.7(3)	O(1)−Cl(1)−O(2)	108.0(4)
Cl(1)−O(4)−Li#3	156.8(6)	O(1)−Cl(1)−O(4)	106.2(3)

2b

Li(1)−N(1)	2.033(5)	N(4)−Li(1′)#4	2.052(5)
Cl(1)−O(1)	1.296(11)	Cl(1)−O(3)	1.292(8)
Cl(1)−O(2)	1.369(11)	Cl(1)−O(3)#5	1.292(8)

N(1)#1−Li(1)−N(1)	109.7(4)	N(1)#1−Li(1)−N(4)#3	111.2(1)
N(1)#1−Li(1)−N(4)#2	107.0(1)	N(1)−Li(1)−N(4)#3	107.0(1)
N(1)−Li(1)−N(4)#2	111.2(1)	N(4)#2−Li(1)−N(4)#3	110.7(4)
O(3)−Cl(1)−O(2)	108.3(6)	O(3)#5−Cl(1)−O(3)	124.2(13)
O(1)−Cl(1)−O(2)	125.2(11)	O(3)−Cl(1)−O(1)	95.9(6)

^{a} Symmetry transformations used to generate equivalent atoms. **1b**: #1 $y, -x + 1, z - 1/4$; #2 $x - 1, y, z$; #3 $-y + 1, x, z + 1/4$. For **2b**: #1 $-x + 1, -y + 1, z$; #2 $-x + 1, y + 0, z - 1/2$; #3 $x, -y + 1, z - 1/2$; #4 $x, -y + 1, z + 1/2$; #5 $x, -y + 1/2, z$.

possible applications in electrical conductors and photosensitive organic devices.[30,31] **2a** was synthesized by the reaction of diimidazolyl ketone with pyrene carbaldehyde in the presence of $CoCl_2·6(H_2O)$ at 80 °C for 2 h.[24,25] Chromatographic purification of the reaction mixture afforded **2a** as an off-white powder which was subsequently characterized

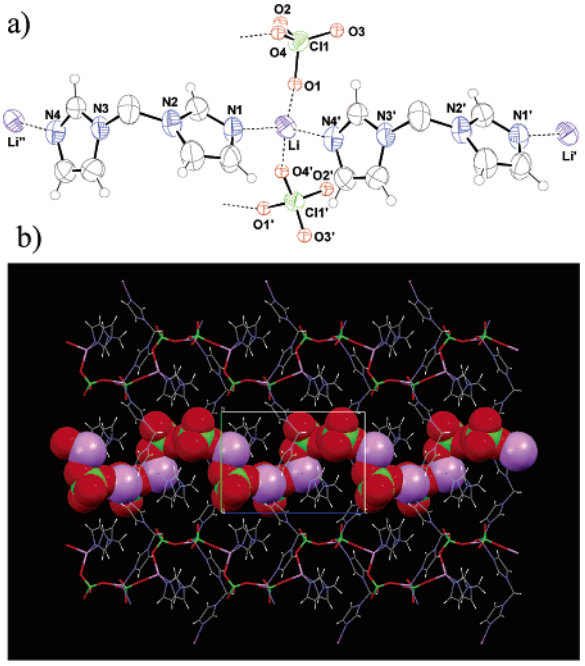

Figure 1. (a) ORTEP view of the Li(Bizm)·ClO_4 molecular structure and the *zigzag* polycoordination structure for lithium ions and bisimidazoles. (b) Unit cell structure of Li(Bizm)·ClO_4 viewed along the b axis, showing a fragment of the helical polystructure formed by the lithium and perchlorate anions.

by ^1H NMR, ^{13}C NMR, and mass spectra analyses. Further, **2a** was dissolved in acetonitrile and was added dropwise to an equimolar solution of $LiClO_4·3(H_2O)$ in acetonitrile for an hour. Subsequent slow evaporation of this solution at 20 °C yielded colorless needle-shaped crystals of $Li·(Pbizm)_2·[ClO_4]·(CH_3CN)$ (**2b**), which were later subjected to X-ray crystallographic investigations.

X-ray Crystal Structures. From the X-ray crystallographic analysis, $[Li(Bizm)]^+[ClO_4]^-$ was found to exist as a tetragonal unit cell with the chiral space group $P4_1$ (a = 9.151(2) Å, c = 13.023(5) Å), which is typical for the helical translation structure because of the inorganic Li salts along the c axis (Figure 1 and Table 1). The Li atom is tetrahedrally coordinated with two nitrogen atoms of Bizm and two oxygen atoms of two $[ClO_4]^-$ anions on either side. The Bizm moieties serve as bridges between lithium atoms forming a *zigzag* pattern, leading to a one-dimensional coordination polychain structure with normal Li···N-distances (2.008(8) Å and 1.997(8) Å). The coordination angle (∠(N1···Li···N4′)) was found to be 108.1°. A single chain of the lithium-bridged polystructure is oriented parallel to the c axis and perpendicular to the next layer with a 1:1 binding ratio of the Bizm ligand to the lithium ion. The anhydrous $LiClO_4$ structure, being a NiAs-type with a 3-dimensional network,[32,33] was found to reorient into helical chains composed of Li^+ and $[ClO_4]^-$ ions with a contact distance of 1.958/2.003 Å for the chain unit (···Li^+·[··O−$Cl(O_2)$ −O··]$^-$···), when complexed with Bizm ligands. Thus, the crystal structure of **1b** is the first example for a

(30) Munakata, M.; Wu, L. P.; Kuroda-Sowa, T.; Maekawa, M.; Suenaga, Y.; Sugimoto, K. *Inorg. Chem.* 1997, *36*, 4903−4905.
(31) Goddard, R.; Haenel, M. W.; Herndon, W. C.; Krueger, C.; Zander, M. *J. Am. Chem. Soc.* **1995**, *117*, 30−41.
(32) Wickleder, M. S. *Z. Anorg. All. Chem.* **2003**, *629*, 1466−1468.
(33) Henderson, W. A.; Brooks, N. R. *Inorg. Chem.* **2003**, *42*, 4522−4524.

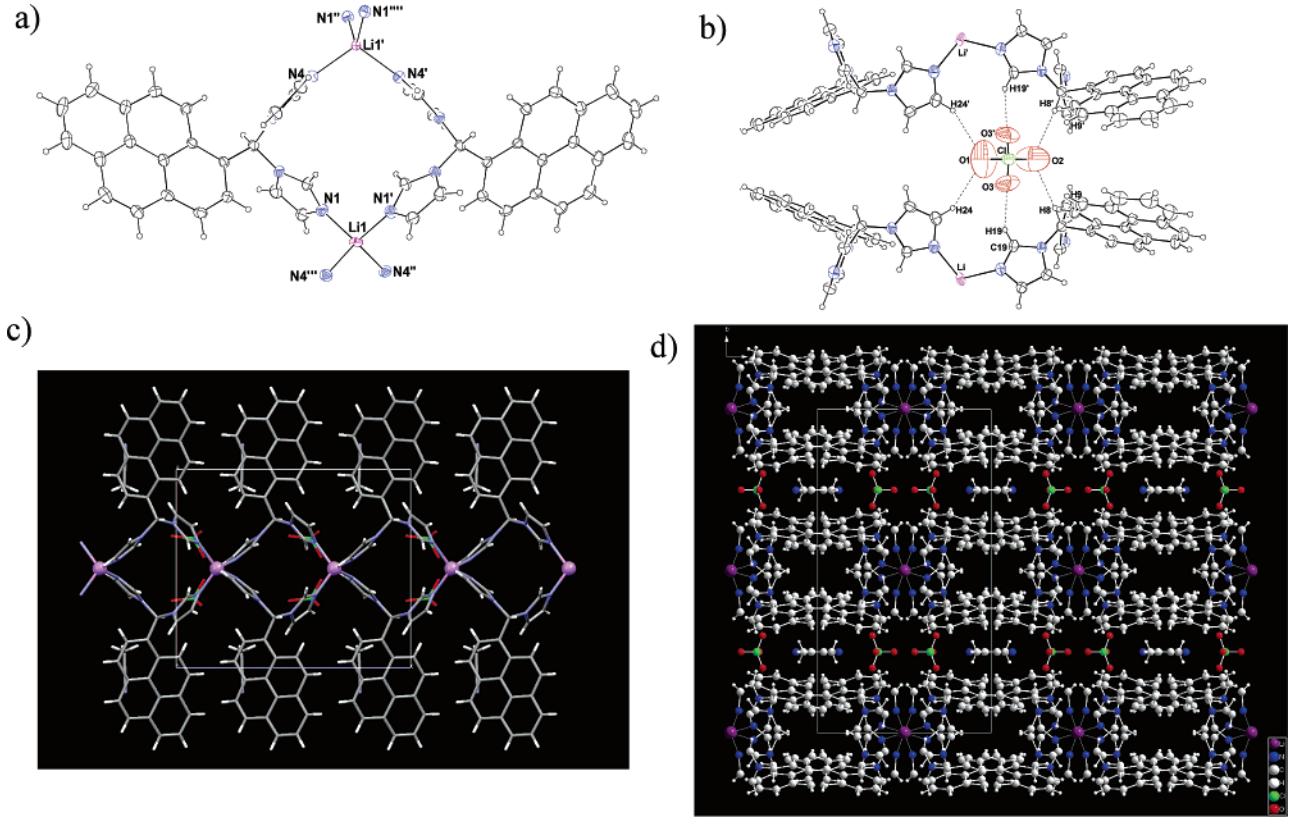

Figure 2. Single-crystal structure of $Li(Pbizm)_2{\cdot}ClO_4{\cdot}(CH_3CN)$. (a) An ORTEP plot of coordination fragments between Li^+ ions and Pbizm molecules along the *c* axis. (b) Section view of $[ClO_4]^-$−Pbizm hydrogen binding structure. (c) Section view of the Li^+−Pbizm chelating 1D-chain structure with the ac plane and the Li^+ pseudochain along the *c* axis. (d) Viewpoint of the *ab* plane showing the layer packing along the *b* axis and the porous formation along the *c* axis. Green, Cl; red, O; pink, Li; blue, N; gray, C.

lithium coordinated helical ionic polystructure which is similar to the vanadium/cobaltoxo hybrid coordination polystructure.[35]

The reaction of **2a** with $LiClO_4{\cdot}3(H_2O)$ yields the coordination polymer $Li{\cdot}(Pbizm)_2{\cdot}[ClO_4]{\cdot}(CH_3CN)$ (**2b**) (Figure 2). It is a noncentric orthorhombic system (*Abm*2), wherein two racemic conformations of Pbizm structures were observed in the unit cell (Table 1). The central Li atom is almost in a regular tetrahedral coordination with four nitrogen atoms of bisimidazole with the coordination distances of 2.032 (Li···N1) and 2.052 Å (Li···N4) and an angle range of 107.0−111.2° (average 109.5°) (Figure 2a). This unique binding mode ultimately yields microchannels in the *c* axis direction, encapsulating a linear array of Li^+ ions. In Figure 2c, one can note a one-dimensional pseudochain structure for Li^+ ions ($Li^+{\cdots}Li^+$ distance = 7.38 Å). The hydrogen-bonding interactions between oxygen atoms of perchlorate and few protons of the Pbizm moiety are strong and asymmetric with the interionic hydrogen bond distances of O(2)···H(18), O(3)···H(19), and O(1)···H(24) being 2.582, 2.563, and 2.711 Å, respectively. This resulted in a distorted tetrahedral geometry of $[ClO_4]^-$ with its oxygen atoms being strongly disordered (Figure 2b). Unlike for **1b**, where Li^+ and $[ClO_4]^-$ reorient into helical polystructures, in **2b** they are separated as individual layers of Li^+ and $[ClO_4]^-$ in the *b* axis direction (Figure 2d)

The unique topology of complex **2b** is simplified in Figure 3. If the (010) plane is considered to be the horizontal one (basal plane), the angle (θ) between the pyrene ring plane and the basal plane is 23.5°. The pyrene moieties that are assembled with the intermolecular $\pi-\pi$- facial interactions orienting parallel to each other are in a V-shaped conformation on either side of the (010) plane with the 2θ angle. This generated porous sections in the architecture, the dimensions for Li-imidazole layers being $l \times A(B) = 4.228 \times 8.13$ (2.53) Å^2 and $l \times C(D) = 8.91$ (3.301) Å^2 for perchlorate/solvent layers (in the split direction *b* axis).

The thermal stability of the complexes was investigated by thermogravimetric analyses (TGA) (Figure 4). Both compounds **1b** and **2b**, in the presence of air or nitrogen, showed high thermal stabilities up to 300 and 250 °C, respectively.

Thermograph Analysis of 1b and 2b. The TGA diagram shows an abrupt weight loss of $Li(Bizm){\cdot}ClO_4$ (**1b**) between 288 and 400 °C which corresponds to ~58.2% loss of Bizm (**1a**), and the decomposition temperature of anhydrous $LiClO_4$ is 430 °C.[38] In the case of $Li(Pbizm)_2{\cdot}ClO_4{\cdot}(CH_3$-

(34) Harris, K. D. M.; Tremayne, M. *Chem. Mater.* **1996**, *8*, 2554−2569.
(35) Zheng, L. M.; Whitfield, T.; Wang, X.; Jacobson, A. J. *Angew. Chem., Int. Ed.* **2000**, *39*, 4528−4531.
(36) Wilcx C. S. In *Frontiers in Supramolecular Organic Chemistry and Photochemistry*; Schneider, H.-J., Dürr, H., Ed.; VCH: Weinheim, Germany, 1991; pp 123−143.
(37) Wang Z.; Enkelmann V.; Negri F.; Muellen K. *Angew. Chem., Int. Ed.* **2004**, *43*, 1972−1975.

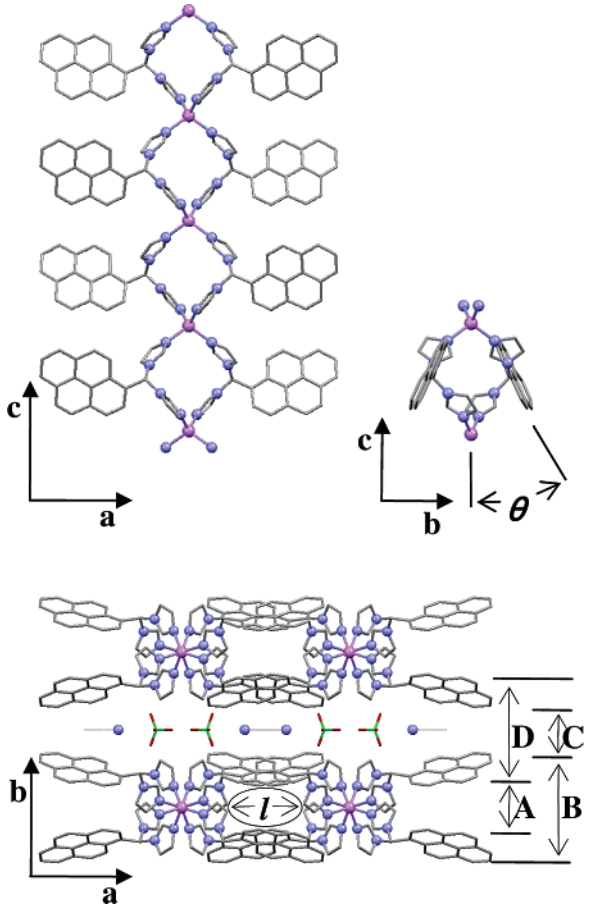

Figure 3. Schematic illustration of $Li(Pbizm)_2 \cdot ClO_4 \cdot (CH_3CN)$ with the porous surrounded by pyrenes.

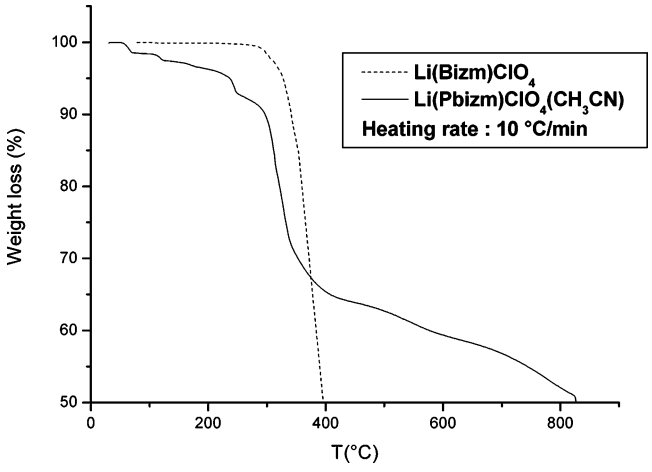

Figure 4. TGA diagram of $Li(Bizm) \cdot ClO_4$ (black dotted line) and $Li(Pbizm)_2 \cdot ClO_4 \cdot (CH_3CN)$ (black solid line).

CN) (**2b**), we observed gradual removal of CH_3CN from 50 to 223 °C with a weight loss of about 4.3%. Pbizm (**2a**) probably decomposes into pyrene and imidazole moieties between 250 and 360 °C, resulting in a weight loss of ~35%, which is contingent on the loss of imidazole moieties. At more than 360 °C, slow removal of black residual carbonyl compounds and lithium salts was observed. Vacuum sublimation (200−220 °C, $<10^{-3}$mbar) of $Li(Bizm)ClO_4$(**1b**) afforded two anhydrous products which were identified as Bizm (**1a**) and $LiClO_4$ by single crystal X-ray diffraction and powder X-ray analysis. It should be noted that anhydrous $LiClO_4$ was synthesized only recently, and its structure was characterized.[32−34]

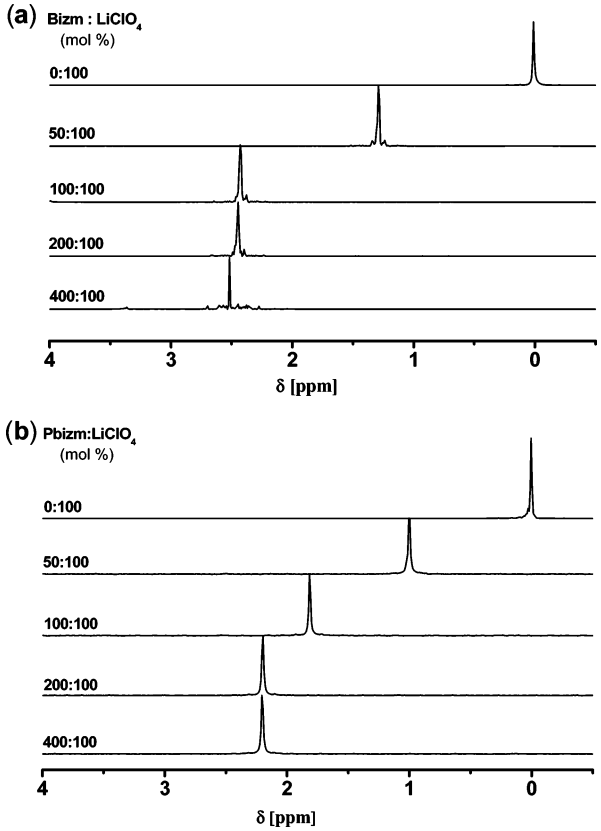

Figure 5. Change of the ^{7}Li NMR chemical shift peaks with the increasing concentration of **1a** (a) and **2a** (b) at 3.75 mM $LiClO_4 \cdot 3(H_2O)/CD_3CN$.

^{7}Li NMR Spectroscopy for Binding Study. The binding properties of Li^+ with **1a** and **2a** were analyzed by monitoring the changes in the chemical shift of the Li^+ ion during ^{7}Li NMR titrations in CD_3CN solution (Figure 5a and b) as an analogy to ^{1}H NMR titrations from our previous papers.[17] The chemical shifts of ^{7}Li NMR were externally referenced to 1 M $LiClO_4 \cdot 3(H_2O)$ in CH_3CN. The addition of an equimolar amount of **1a** and twice the equimolar amount of **2a** to $LiClO_4$ (3.75 mM in acetonitrile) induced large downfield chemical shifts ($\Delta\delta$ = 2.49 and 2.19 ppm, respectively) of the Li^+ ion. There is no significant change in the chemical shift beyond the 1:1 molar ratio of **1a** to Li^+ and the 2:1 molar ratio of **2a** to Li^+. The lesser change in the chemical shift for Li in the presence of **2a** would be attributed to the steric effect of the pyrene moiety which lies at the vicinity of the imidazole moieties.

The association constant (K_a), calculated with the HOSTEST program,[36] for the Li^+ ion with **1a** was found to be $K_a = 2.81 \times 10^5$ M^{-1} and that with **2a** is $K_1 = 1.48 \times 10^4$ M^{-1} and $K_2 = 620$ M^{-1} (Figures 6 and 7). Therefore, the binding pattern of **2a** with the Li^+ ion in CH_3CN is 1:1 at the lower concentration of **2a**, while it changes to 2:1 with the higher concentration of **2a**. It is quite likely that the $\pi-\pi$

(38) Watson M. D.; Fechtenkoetter A.; Muellen K. *Chem. Rev.* **2001**, *101*, 1267−1300.

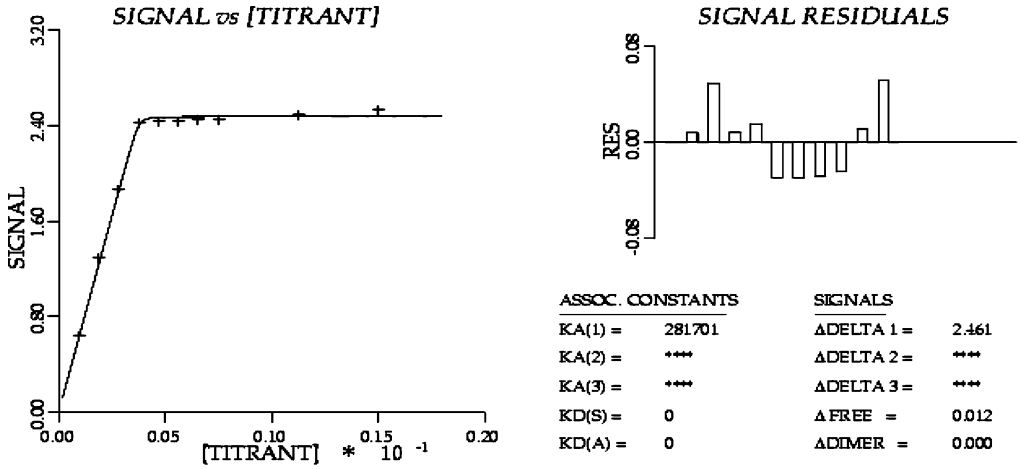

Figure 6. ^{7}Li NMR titration curve for the receptor **1a** and Li^{+} in CD_3CN. Theoretical curve fitting of the experimental data shows a 1:1 binding profile. [Li^{+}] = 0.00375 M as fixed concentration. [**1a**] = 0−0.016 M.

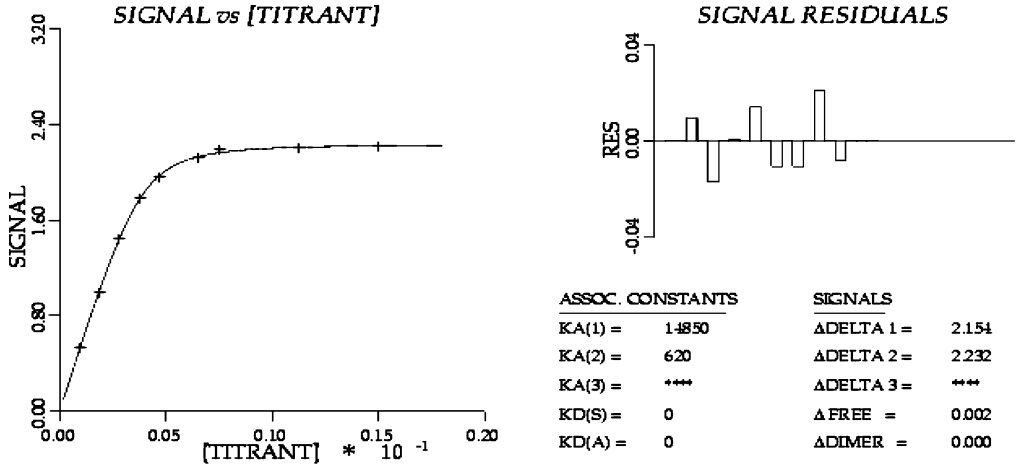

Figure 7. ^{7}Li NMR titration curve for the receptor **2a** and Li^{+} in CD_3CN. Theoretical curve fitting of the experimental data shows a 2:1 binding profile. [Li^{+}] = 0.00375 M as fixed concentration. [**2a**] = 0−0.015 M.

facial interaction between pyrene groups occurs at the higher concentration of **2a**. In fact, we observed that 2:1-type single crystals were formed and isolated in the condensation state in solutions of varying molar ratios (2:1 and 4:1) of **2a** to $LiClO_4$ in CH_3CN.

Therefore, the Li ions are firmly attached to the lone electron pairs of the imidazole nitrogens, indicating a strong electrostatic interaction and a more or less rigid stabilization of the Li ions inside the Bizm network. The fact that Li^{+} in **2b** is coordinated by two ligands (four nitrogen lone pairs) further supports the notion that in the liquid state the separation of the ionic fragments prevails, a feature which is otherwise commonly not observed. Thereby, the ionic channels in the solid crystal resemble those in the liquid state.

Electrical Properties. The ionic conductivities of $LiClO_4 \cdot 3(H_2O)$ in CH_3CN without and with the presence of **1a** and **2a** were measured at room temperature. The ionic conductivity of a 1.0 mM $LiClO_4 \cdot 3(H_2O)$ in CH_3CN solution was indicated by the value 9.20 mS/cm. It was observed that the conductivity of 0.2 mM $LiClO_4 \cdot 3(H_2O)$ was reduced from 2.84 mS/cm to the lower values when the concentration of **1a** and **2a** was increased in the CH_3CN solution (Figure 8). The ionic conductivity curves constantly change before the 1:1 molar ratio for Bizm (**1a**) and the 2:1 for Pbizm (**2a**)

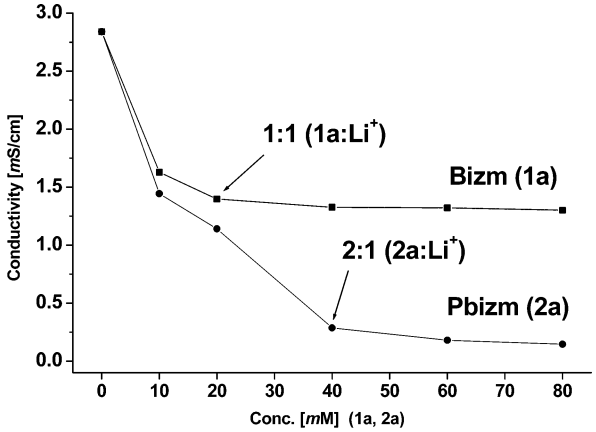

Figure 8. Ionic conductivities of $LiClO_4 \cdot 3(H_2O)$ with the serial molar ratios for Bizm (**1a**) and Pbizm (**2a**) in CH_3CN. $c(LiClO_4)$ = 0.20mM.

with Li^{+}, and thereafter, there is no significant change in the ionic conductivity. The trend in the conductivity measurement is in good agreement with the ^{7}Li NMR binding study and X-ray structure analysis.

Figure 9 shows cyclic voltammograms (CVs) for a $LiClO_4 \cdot 3(H_2O)$ (0.25mM) with the various molar ratios for Bizm (**1a**) and Pbizm (**2a**) in CH_3CN. Clearly, a simple wave reversible redox system sweeps in a wider potential range

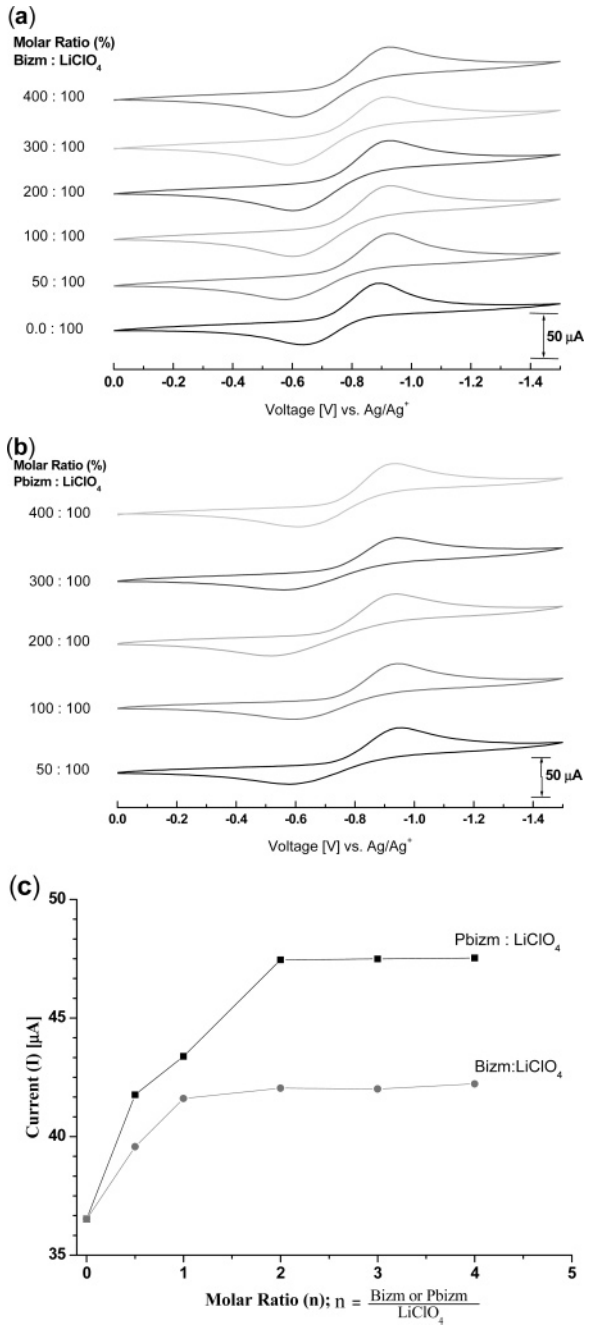

Figure 9. Cyclic voltammograms of $LiClO_4$ (0.5mM) were recorded in 0.4 M $TBAPF_6$ and CH_3CN, in the presence of Bizm (**1a**) (a) and Pbizm (**2a**) (b) with molar ratios (%) of 0.0, 50, 100, 200, 300, and 400 and a scan rate of 50 mV/s. (c) Current vs molar ratio for Bizm and Pbizm to $LiClO_4$.

(0 to −1.5V) at the scan rate of 50 mV/s. Bizm and Pbizm show interesting electrochemical changes in the binding study between the Li^+ ion and Bizm/Pbizm. The electrical data of cyclic voltammograms are in Table 3. The reduction and oxidation potential peaks (E_{pc} and E_{pa}) appeared near −0.604 and −0.920 V, respectively, for a Bizm/$LiClO_4$·3(H_2O) system and near −0.596 and −0.926 V, respectively, for a Pbizm/$LiClO_4$·3(H_2O) system. We noticed that there is no clear shifting in the redox potential peaks (E_{pc} and E_{pa}) at various molar ratios of Bizm (**1a**) and Pbizm (**2a**) to the Li^+ ion. The redox potential (E_0) of the Bizm/Li^+ system shows the lowest value (−0.319 V) at the 1:1 molar ratio. The Pbizm/Li^+ system shows the lowest value (−0.411 V) at the 2:1 molar ratio. In the reversible redoxsystem ($i_{pc}/i_{pa} = 1$), after every 10 cyclic voltammograms, we analyzed the change in the current densities (i_{pc} and i_{pa}) resulting from the increased molar ratios for Bizm (**1a**) and Pbizm (**2a**). The transformation curves for the current densities were approximately saturated after molar ratios of 1:1 for Bizm and 2:1 for Pbizm. Therefore, the stoichiometric binding patterns reflected by the ^7Li NMR titration are clearly reflected in the ionic conductivity measurement of Li ion and cyclic voltammogram.

Table 3. Cyclic Voltametric Redox Potential and Current for the Molar Ratio of Bizm (**1a**)/Pbizm (**2b**) to Li^+ in the Solution of CH_3CN with 0.25 mM $LiClO_4$·3(H_2O)[a]

	molar ratio	E_{pc} (mV)	E_{pa} (mV)	E_0 (mV)	$E_{1/2}$ (mV)	I_{pc}, I_{pa} (μA)	i_{pc}/i_{pa}
[Li^+]	0.0	−642	−891	−249	−766.5	36.52	1.000
Bizm (**1a**)	0.5	−567	−928	−361	−747.5	39.57	
	1.0	−604	−923	−319	−763.5	41.60	
	2.0	−607	−928	−321	−767.5	42.04	1.000
	3.0	−597	−923	−326	−760.0	42.01	
	4.0	−604	−928	−324	−766.0	42.22	
Pbizm (**2a**)	0.5	−589	−953	−364	−771.0	41.76	
	1.0	−596	−933	−337	−764.5	43.38	
	2.0	−523	−934	−411	−728.5	47.45	1.000
	3.0	−565	−938	−373	−751.5	47.49	
	4.0	−615	−929	−314	−772.0	47.53	

[a] Supporting electrolyte conditions: Bizm and Pbizm, 0.25mM; $LiClO_4$·3(H_2O), 0.5mM; [*n*-Bu_4N]PF_6, 0.4M; scan rate, 50 mV s^{-1}; scan range, 0 to −1.5 V; $E_0 = E_{pa} - E_{pc}$, $E_{1/2} = (E_{pa} + E_{pc})/2$.

Under the typical conditions of various molar ratios in the CH_3CN solution, the ligand compounds (Bizm (**1a**) and Pbizm (**2a**)) have influence only on the current changing for the electrochemical reaction of lithium salts (Figure 9c). In addition, the thermal stability of the compounds observed at even higher temperatures clearly demonstrates that carefully designed bisimidazole derivatives with weakly coordinating anions to Li^+ could trigger potential applications in the field of Li ion batteries. Additionally, suitably substituted aromatic/aliphatic functional moieties in the connecting CH_2 group of the bisimidazole could enhance the thermal stability and physicochemical properties of the newly designed and synthesized compounds.

IV. Conclusion

We have synthesized two lithium-based organic−inorganic hybrid materials with interesting topochemical properties. In both cases, lithium exhibits unusually high binding affinity toward the nitrogen atoms of bisimidazole moiety. The presence of a substituent group at the bridging carbon of the bismidazole moiety plays a crucial role in determining the stoichiometry of these compounds in solution and in the condensed state. Unsubstituted Bizm (**1a**) preferred a 1:1 stoichiometry, whereas in Pbizm (**2a**), the ratio is 2:1 with Li^+. In the crystal structure of Pbizm (**2b**), we have observed the controlled ion separation and ion channel formation resulting from the chelation of imidazole moieties with a linear array of Li ions and the rearrangement of pyrene moieties. It can be inferred that the artifical design of molecular crystals and liquid crystalline hybrid materials

modifies the unusual building blocks to the self-assembled helical columnar packing of polycyclic aromatic hydrocarbons.[31,37,38] The results bode well for the future generation of hybrid materials containing functionalized bisimidazoles, whose properties could easily be fine-tuned by varying the nature of substitutents inherent to the bisimidazole moiety.

Acknowledgment. We thank Prof. S. M. Park and Prof. M. H. Rhee for their useful information on data characterization and analysis. This work was supported by GRL project (KOSEF/MOST), Postech BSRI research fund 2006, and BK21.

Supporting Information Available: CIF files for compounds **1b** and **2b**·(CH_3CN). This material is available free of charge via the Internet at http://pubs.acs.org. Crystallographic data for the structures reported in this paper have been deposited with the Cambridge Crystallographic Data Centre as supplementary publications CCDC-285304 (**1b**) and CCDC-285305 (**2b**). Copies of the data can be obtained free of the charge via www.ccdc.cam.ac.uk/conts/retrieving.html (or from the Cambridge Crystallographic Data Centre, 12 Union Road, Cambridge CB21EZ, UK; fax (+44)1223-336033; e-mail deposit@ccdc.cam.ac.uk).

IC060323H